Final Report
Covering Period: April 15, 2001 to April 30, 2013
Date of Report: May 14, 2013

Award Number:	DE-FC26-01CH11079
Project Title:	Advanced Natural Gas Reciprocating Engine(s)
Project Period:	4/15/01 – 4/30/13
Recipient Organization:	Caterpillar Inc.
Partners:	Not Applicable
Technical Contact:	Doris Kwok 14009 Old Galena Road Mossville, IL 61552-7547 Phone: 309-494-2685 Fax: 309-578-9900 Email: Kwok_Doris@cat.com
Business Contact:	Cheryl Boucher 14009 Old Galena Road Mossville, IL 61552-7547 Phone: 309-578-9961 Fax: 309-578-4113 Email: Boucher_Cheryl_D@cat.com
DOE Project Officer:	Walt Parker Phone: 412-386-7357 Email: walter.parker@netl.doe.gov
DOE Project Monitor:	Not assigned
DOE HQ Contact:	Not available
DOE Contract Specialist:	Jodi Collins Telephone: 304-285-1390 Email: jodi.collins@netl.doe.gov

Acknowledgment: This material is based upon work supported by the Department of Energy (National Nuclear Security Administration) under Award Number DE-FC26-01CH11079

Summary

Energy independence and fuel savings are hallmarks of the nation's energy strategy. The advancement of natural gas reciprocating engine power generation technology is critical to the nation's future. A new engine platform that meets the efficiency, emissions, fuel flexibility, cost and reliability/maintainability targets will enable American manufacturers to have highly competitive products that provide substantial environmental and economic benefits in the US and in international markets. Along with Cummins and Waukesha, Caterpillar participated in a multiyear cooperative agreement with the Department of Energy to create a 50% efficiency natural gas powered reciprocating engine system with a 95% reduction in NOx emissions by the year 2013. This platform developed under this agreement will be a significant contributor to the US energy strategy and will enable gas engine technology to remain a highly competitive choice, meeting customer cost of electricity targets, and regulatory environmental standard.

Engine development under the Advanced Reciprocating Engine System (ARES) program was divided into phases, with the ultimate goal being approached in a series of incremental steps. This incremental approach would promote the commercialization of ARES technologies as soon as they emerged from development and would provide a technical and commercial foundation of later-developing technologies. Demonstrations of the Phase I and Phase II technology were completed in 2004 and 2008, respectively. Program tasks in Phase III included component and system development and testing from 2009-2012. Two advanced ignition technology evaluations were investigated under the ARES program: laser ignition and distributed ignition (DIGN). In collaboration with Colorado State University (CSU), a laser ignition system was developed to provide ignition at lean burn and high boost conditions. Much work has been performed in Caterpillar's DIGN program under the ARES program. This work has consisted of both modeling and single cylinder engine experiments to quantify DIGN performance. The air handling systems of natural gas engines dissipate a percentage of available energy as a result of both flow losses and turbomachinery inefficiencies. An analytical study was initiated to increase compressor efficiency by employing a 2-stage inter-cooled compressor. Caterpillar also studied a turbo-compound system that employs a power turbine to recover energy from the exhaust gases for improved engine efficiency. Several other component and system investigations were undertaken during the final phase of the program to reach the ultimate ARES goals. An intake valve actuation system was developed and tested to improve engine efficiency, durability and load acceptance. Analytical modeling and materials testing were performed to evaluate the performance of steel pistons and compacted graphite iron cylinder head. Effort was made to improve the detonation sensing system by studying and comparing the performance of different pressure sensors. To reduce unburned hydrocarbon emissions, different camshafts were designed and built to investigate the effect of exhaust valve opening timing and value overlap. 1-D & 3-D coupled simulation was used to study intake and exhaust manifold dynamics with the goal of reducing load in-balance between cylinders. Selective catalytic reduction with on-board reductant generation to reduce NOx emissions was also engine tested.

An effective mean to successfully deploy ARES technologies into the energy markets is to deploy demonstration projects in the field. In 2010, NETL and Caterpillar agreed to include a new "opportunity fuel" deliverable and two field demonstrations in the ARES program. An Organic Rankine Cycle system was designed with production intent incorporating lessons learned from the Phase II demonstration. Unfortunately, business conditions caused Caterpillar to cancel this demonstration in 2011. Nonetheless, Caterpillar partnered with a local dealer to deploy an ARES class engine using syngas from a biomass gasifier as the

primary combustion fuel in Gleason, TN. Upon the successful start-up and commissioning of the demonstration unit, ownership of the system was transferred to the dealer. In order to further our understanding of syngas combustion, a fundamental combustion study on syngas combustion at high pressure and lean condition was conducted through the collaboration with University of Southern California. A Methane program was also developed to rate engine performance for various compositions of syngas using empirical data obtained at CSU.

While much work remains in terms of extending and integrating these developments into commercial products, it is evident that engine manufacturers on our own or through private consortium efforts could not have overcome the financial hurdles to drive these improvements into reciprocating engine and system capabilities, helping maintain the natural gas reciprocating engine power generation technology as a strong option for electric power markets, both in the United States and worldwide.

Introduction

Market demand for reciprocating natural gas engines used in electrical power applications has increased dramatically over the last two decades, and is expected to continue through the foreseeable future. At the same time, continual reductions in emissions output, along with customer demands for increased efficiency, reliability, durability, and lower owning and operating costs have created a need for an improved engine system design. The US Department of Energy, in concert with US manufacturers, created the ARES program in 2001. This program has an ambitious goal of 50% brake thermal efficiency and 0.1 grams of NOx output by the year of 2013. The intent of this competitively funded program is to promote the state of development of advanced engine technologies for integration into advanced natural gas reciprocating engine used in power generation.

The program objectives are to be met in three specific phases:

Phase I	44% Efficiency	0.5 g/bhp-hr NOx
Phase II	47% Efficiency	0.1 g/bhp-hr NOx
Phase III	50% Efficiency	0.1 g/bhp-hr NOx

Phase I was the base program to build a new concept of ARES prototype engine to achieve baseline efficiency and emission targets. Phase II took this base product and extend its efficiency by an additional three points while achieving the program basic NOx emission target. Phase III will either use a larger bore and power product to reach ultimate ARES targets with emissions at or below ARES targets, or to continue to stretch the new ARES platform towards Phase III efficiency and emissions.

This final report describes and summarizes the total work performed. A summary of the Phase I and Phase II demonstrations is first presented followed by a comprehensive description of the results achieved in Phase III.

Phase I Demonstration

The Caterpillar ARES program has developed improvements in power density and fuel consumption that have delivered substantial improvement in owning and operating costs thereby improving the economics of distributed power generation using reciprocating gas engines. In 2004, with the “Raptor” fuel control valve, liquid cooled valve seats, liquid cooled spark plug sleeve, pre-chamber spark plug, high power-density combustion system, optimized after-cooler, optimized detonation detection and the “Charge Density” Air/Fuel ratio control algorithm, the G3520C/E engine demonstrated 44% thermal efficiency and a 0.5g/bhp-hr NOx emissions level. As of 2009, more than 3.84 gigawatts of ARES technology have been deployed worldwide.

Phase II Demonstration

After the phase I demonstration, Caterpillar investigated numerous component technologies to improve overall efficiency. In 2008, with the Organic Rankine Cycle (ORC) machine fully commissioned and the G3520C engine modified to improve its efficiency, Caterpillar demonstrated over 47% thermal efficiency at 1800 rpm. With the internal efficiency enhancements the engine demonstrated 42% efficiency at 1800rpm. With the addition of 220 kW of electric power, over 47% efficiency at 1800rpm was demonstrated. ORC power output as high as 276kW was demonstrated which was well shy of the 350kW design point. It was decided that further improvements will not be investigated until the ORC system is reconfigured for the Phase III efficiency demonstration. A 0.1g/bhp-hr NOx emissions level was demonstrated using the SCR with on-board reductant generation in 2007.

Phase III

Program tasks in Phase III focused on meeting the ARES program goal of 50% thermal efficiency. The intended system would utilize a variety of technologies and efforts were made to investigate meeting the 50% efficiency without the use of the ORC. Projects in Phase III geared toward research of technologies for inclusion in new engine platforms as well as updates of the G3500. The major change in 2011 was the change of the base engine platform of G3500C/E to G3500/CG170.

Laser Ignition

Laser ignition has the potential to provide a high-power ignition source that is robust against extinction, voltage independent, and does not suffer from erosion, thereby allowing reliable operation at lean (lambda > 2.0), high boost conditions (BMEP > 24 Bar) without flashover. This research effort carried out at Colorado State University (CSU) comprised engine-tests to examine performance and operational limits of technologies, as well as research and development into novel fiber optic, multiplexing, and laser source technologies.

In the beginning of 2009, a proven solution was in place with coated hollow core fibers, which form the basis of ongoing engine tests. Additionally, the research team also considered other novel fiber options such as the step-index silica fibers. The first tests examined 100 μm core fibers of length 2 m. To investigate the effect of a larger cladding, CSU measured a step-index fiber with core of 100 μm and cladding of 660μm (large clad-to-core ratio of 6.6:1). The output beam quality was M^2=1.4 for straight configurations (optimum for w/a=0.92) and M^2=2.2 for bent configurations (radius of curvature of 20 cm). These results were promising since they showed that the large clad diameter does indeed improve output beam quality and therefore suggested a method towards fiber delivered laser ignition using these fibers (note that low values of M^2 correspond to high beam quality). CSU continued with a matrix of comparison between several commercial fibers that may allow delivery of laser beams with relatively high output beam quality. The following types of fibers were compared: baseline fiber, fiber with reduced numerical aperture (lower acceptance/exit angle), fiber with thick cladding, and fiber with graded index profile. Tests of each of these fibers, in both straight and bent configurations, were completed. The results suggested that the fiber with thick cladding may be the most effective fiber candidate. Before the end of 2009, CSU combined the step-index fiber approaches with innovative approaches based on using shorter wavelengths. It was found that the breakdown thresholds (to create a spark in atmospheric air) for 355 nm light is ~20 GW/cm^2 compared to ~150-300 GW/cm^2 at 1064 nm. Further, CSU was able to form laser sparks with pulse energies as low as 1-2 mJ at these shorter wavelengths. Although these energies provide sparking, they do not have enough energy content to achieve minimum Ignition energy and ignite lean mixtures. CSU also conducted high power tests with the ultraviolet (355 nm) laser beams and high peak power experiments on 2 m long, 200 micron core, and 745 micron cladding fiber with a loop of 25 cm radius. 1.6 mJ (10 ns) pulses of 355 nm light was able to transmit through the fiber with 1.1 mJ at the output and output beam quality of M^2=10. These parameters are close (within a factor of~3) of those required for spark formation.

In the beginning of 2010, experiments for a 2m long solid core step index silica fiber of 200 μm core/ 745 μm cladding (and a loop radius of 25 cm radius) showed output beam quality of M^2 < 4 using 633 nm. These output M^2 values are less than would be obtained with conventional silica fibers of the same core size indicating superior beam quality. The high beam quality, which aids in spark formation, is due to the unusually thick cladding that yields a more rigid core-cladding interface resulting in less mode coupling. CSU also examined the optimum laser wavelength, i.e. the tradeoffs between 355 nm and 1064 nm light (both

available from Nd:YAG lasers). The focus was on 1064 nm light, which has the practical advantage of lower cost laser sources relative to 355 nm. Spot diameters achievable were measured with the high quality beams of 1064 nm light (after fiber exit) and the measured spot diameters of 9 – 10 μm with a plano-convex lens of 9 mm focal length, for which it was estimated that the pulse energies required for sparking (i.e. for focal intensities > 300 GW/cm^2) to be 2.5 – 3 mJ. Since the silica fibers have higher damage thresholds for 1064 nm light compared to 355 nm light, these energies should be possible with 200 μm fibers.

In 2010, CSU succeeded in using 2 m long 400 μm core fibers to deliver laser sparks at atmospheric pressure air (0.85 bar at Fort Collins) with 10 ns pulse and 1064 nm light. The team was able to achieve 100% spark formation at 10 Hz with 3 – 4 mJ pulse energies at 10 Hz with the fiber held at a relatively straight configuration. This result provided the first demonstration of spark delivery through conventional step index silica fibers and represents a major research milestone owing to the excellent bend performance and long lifetimes that these fibers can potentially provide. Tests were also conducted with these fibers in coiled configuration (with a loop of 25 cm radius). The coiled fibers resulted in decreased output beam quality (M^2~4.5) and hence the achievable focused spot dimension was higher (12 μm). Testing was also conducted to examine the ability to form sparks through these coiled fibers at higher ambient pressures. Although the coiled configuration did not spark at atmospheric pressure, 100% spark formation at just 0.7 bar (gauge pressure) with 3 mJ pulse energies was obtained. It was also found that the required pulse energy for 100% sparking was reduced from 3 mJ to 1.5 mJ as the cell pressure was increased from 0.7 to 6.9 bar. These tests conducted at high pressure suggest that these fibers should be able to deliver sparks reliably and easily at high motored pressures in the engine cylinders. As part of this research effort, CSU also designed and manufactured a test setup for investigating the effects of vibrations on the performance of the laser fiber delivery system (see Appendix A).

In 2011, CSU designed a compact optical spark plug for use with fiber delivered laser ignition on the CFR engine. The optical plug is shown in Figure 1. It has the capability, via an adjustment plate at its input side, to optimize the alignment of the fiber output laser beam with the optical axes of the lenses. The optical fiber is connected to the optical spark plug by a standard SMA connector allowing easy connection (and fiber replacement). The laser beam from the fiber is first expanded by a diverging lens (Lens 1) and then collimated by a second lens (Len 2). Finally, the collimated beam is focused by a 10 mm focal length Gradium lens (Lens 3) through a 3 mm sapphire window. The use of the 3-lens system, with diverging lens, allows the overall system to be more compact (as opposed to letting the fiber exit beam diverge on its own with no diverging lens). The sapphire window is held between two copper O-rings and is held firmly within the spark plug by a threaded insert. The optical spark was successfully tested to withstand high pressures. The overall length of the spark plug is approximately 6 inches.

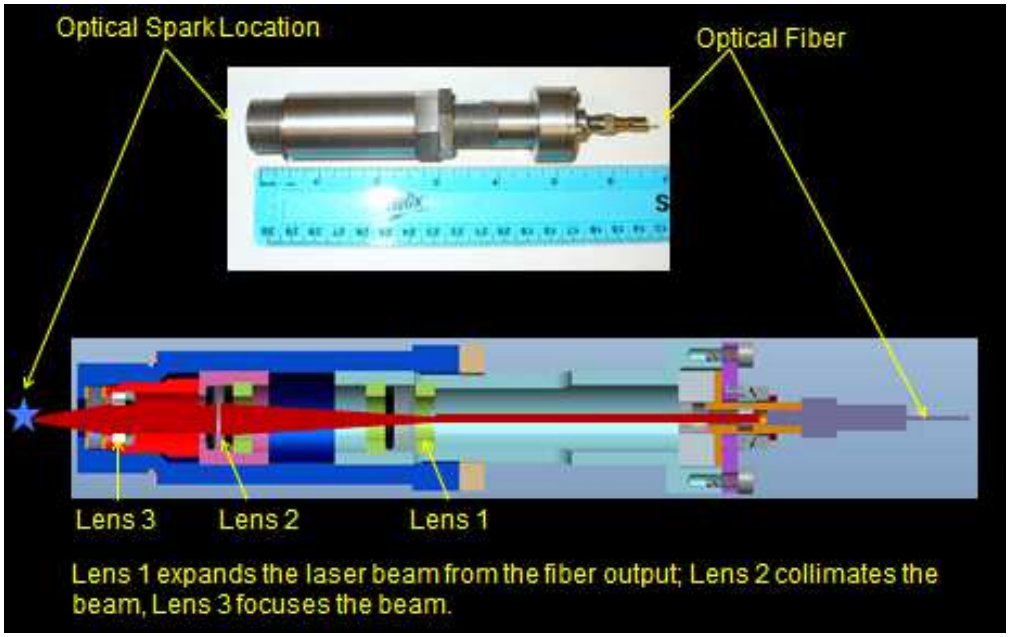

Figure 1: Optical spark plug for testing on CFR engine. Top: Photograph of the optical spark plug. Bottom: Cross-sectional drawing of the optical spark plug.

CSU tested the full fiber delivered laser ignition system configuration as required for testing on the CFR engine. A Nd:YAG laser (Continuum Model 8000) was used for the experiments. CSU simulated on the bench-top the way the fiber and the spark plug will be mounted on the CFR engine. For simulating engine conditions on the bench-top, the optical spark plug was connected to a high-pressure chamber to test spark formation in the pressurized gas (100 psi) of the chamber. The full system in this configuration was able to deliver laser beam with M^2=3 thereby enabling reliable sparking at 100 psi with input energies of 15 mJ. The transmission efficiency of the fiber was measured at 85%, while the transmission of the entire system (after the optical spark plug window) was measured at 70%, both values consistent with expectations. By the end of 2011, an engine test was performed using a CFR engine with a compression ratio of 14:1, located at CSU. The test involved comparing engine performance for ignition by an electrical J-gap spark plug and ignition by the laser system. At the engine speed of 950 rpm and Net Mean Effective Pressure levels of 6, 8, 10 and 12 bar, the laser ignition system stably delivered 7mJ ignition energy and demonstrated lean burn performance. When comparing laser ignition to ignition by a conventional spark plug, this engine test did not fully validate laser ignition system delivered superior ignition performance because the COV of IMEP, NOx level and fuel efficiency was better in some operating conditions, but worse in other operating conditions. It was partly due to the limitation of maximum ignition power related to the fiber optics damage, and the effect from vibration that deteriorated the quality of the laser beam.

Distributed Ignition

This work was initiated because a production viable ignition system for use at power densities above 20 bar BMEP had not been identified and Distributed IGNition (DIGN) is among the best alternatives. In 4Q2009, the design of a multi-cylinder metering system was underway and modeling of the flow delivery was complete. In 1Q2010, the cylinder head

modification to facilitate port visualization was completed and the preliminary test for DIGN visualization was completed on a non-engine test fixture. The objective of the preliminary test was to investigate the DIGN phenomena with more controllable environment and find out the potential issues on visualization before progressing to the single cylinder engine test. Visualization design issues were found and resolved during these early tests.

The single cylinder engine testing examined the oil flow from the injection site to the combustion chamber. A cylinder head with a quartz window was used to examine oil injection and oil flow in the intake stream under actual running conditions. A second cylinder head was equipped with an endoscope and a port for laser light to investigate the characteristics of DIGN combustion in cylinder. The visualization research completed has delivered clear high-speed images of oil injection and oil droplet ignition in cylinder. The video results of this testing aided in the direction of future modeling and provided a better understanding of the DIGN phenomena.

During the remainder of 2010, production ready type DIGN injectors were designed and prototypes procured for Single Cylinder Test Engine (SCTE) and multi-cylinder engine testing. Delivery variations were found to be within 3 ~ 5% range with oil temperatures, delivery tube diameters, oil inlet pressures, current signal and intake port pressure. Single cylinder testing was performed with a new DIGN injector design. However, a cost benefit analysis showed that the fuel savings for using DIGN do not offset the cost of additional oil. As a result, DIGN was put on hold until the economics change or the additional benefits of ignition system life could be realistically tapped.

Turbocompound

In 2009, Caterpillar initiated the analysis of an electric turbocompound system, which may utilize either an integral generator/turbocharger, or a separate turbine/generator. The cost of both the generator and the power electronics to condition the generator output is expected to decline rapidly as variable frequency power conditioning becomes more widespread in the aerospace, microturbine, alternate energy, and heavy equipment segments. With the expected cost decline, turbocompounding can be an attractive method of providing additional power and therefore improving engine efficiency, while retaining some of the exhaust heat for Combined Heat and Power applications. Estimates of the net efficiency gain for the turbocompound system are approximately 3% points, after accounting for the combustion effects and pumping losses due to high backpressure.

The coupling of the power recovered using a turbocompound could be captured by mechanically connecting the turbocompound to the crankshaft of the engine using a viscous damper and a gearbox. The power could also be used to drive a stand-alone high-speed generator, providing a less intrusive solution often called Electric Turbo Compound (ETC). In order to compare mechanical and electric turbocompounding, a study was conducted to investigate the feasibility of the power conditioning system (PCS) for an ETC.

A statement of work was established with internal resources to complete a literature review and thermodynamic analysis. This work leveraged the analysis and models developed during the Aggressive Miller Cycle analysis. Due to resource constraints, the project was not advanced during 2009.

A new team was assembled and work was resumed in 2010. SCTE data was analyzed via study of the exhaust pressure versus intake pressure. These values were used in a simulation to understand the relationship between inlet manifold air pressure (IMAP), exhaust manifold air pressure (EMAP) and their impact on residual gas fraction. The

simulation was then used to determine the EMAP sweep of interest to simulate the extremes of turbocompound engine operation on the combustion in the SCTE.

The impact of increased and decreased amounts of valve overlap was also identified as an area critical to understanding the optimum application of turbocompound to a gas engine. Two camshaft configurations were identified to cover the overlap range of interest in future SCTE work. A second statement of work was established to investigate the feasibility of the PCS project. Two topologies, two levels (2L) and three levels (3L), for the front end of the power converter were proposed for the PCS. A commercially available insulated-gate bipolar transistor (IGBT) block was identified. A simulation was performed on each topology using selected IGBT blocks. The results showed that the 3L topology has higher efficiency and thus less cooling requirement, while it has higher number of devices.

Three-phase inverter topology was selected based on literature review, simulation results, and ease of control. The control was tested on a 150KVA inverter with less than 2% THD and good load stiffness. Infineon 600A IGBT was selected for the potential prototype build. Three high-speed generator suppliers were contacted and notified for the upcoming request for proposal from CAT ETC work. The functional specification of the high-speed generator was drafted.

The rectifier control was developed and tested, which converts 3-phase AC to regulated DC voltage. The rectifier works with various types of generator (induction, surface and interior permanent magnet) and utility grid. Besides, as a test bed for ETC concept, a 150kVA PCS system was built and commissioned in a test cell.

In 2Q2010, the camshafts identified during previous engine simulation work, as providing a better breathing solution for a turbocompounded engine, were procured and inspected. The camshafts would later be used during single cylinder engine evaluation along with the standard cam in an effort to understand their impacts on net power increase of the turbocompound engine system at various loads and levels of backpressure.

As a test bed for ETC concept, a 150kVA PCS system was commissioned. The rectifier control was tested using the power from a Surface PM (Permanent Magnet) generator and utility grid. The rectifier was able to solidly regulate the DC bus voltage as requested. Additionally, a bidirectional DC-DC converter (BDC) was installed and tested. The BDC is able to charge and discharge energy from a battery bank. The BDC was an option for assisting the gas engine during step load. A review of the costs of the components of an electrical turbocompound system was held with the supplier. The total system costs for the ETC approach that was most affordable was still on the order of 3X the cost of the similar mechanical turbocompound system. In light of this Caterpillar decided not to pursue the ETC options and would instead focus on the mechanical turbocompound approach and its value analysis.

Later in 2010, design concepts of an axial turbocompound turbine and a radial turbine were created. The axial turbine concept was abandoned as the packaging of this type of turbine proved to be much more cumbersome than that of the radial turbine and offered no performance advantage in this application. The component costs for the mechanical system were estimated with the hot turbine components representing about 2/3 of the total cost. Early single cylinder engine testing of the turbocompound operating conditions resulted in unstable operation due to deterioration in the required control elements – fuel valve and exhaust backpressure valve. Both the mechanical and software elements of the control system were rebuilt. Testing was completed on the SCTE with the hardware configuration of the G3500E+ engine before the end of 2010. Tests were run using the standard camshaft along with others with lesser and greater amounts of valve overlap in order to study the

impact on unburned hydrocarbons. Backpressure applied to the engine exhaust system simulated the conditions that would be imposed by the use of a turbocompound turbine. Results indicated a large (and expected) pumping work penalty associated with the backpressure and larger benefits from the turbocompound power harvested from the exhaust stream along with a benefit of more complete combustion of the fuel in the combustion chamber. The net benefits from the use of turbocompounding behind the E+ engine are estimated to be a power increase of 300 kW on top of the base rating of 2000 kW, resulting in a net efficiency improvement of 3 points. The original concept design work was completed with the expectation that we would only see 150 kW from the turbocompound system so the hardware was not sized properly for the 300 kW power level. Although the efficiency improvement realized by the use of turbocompound did not match that of the ORC system, the cost/benefit ratio of the technology appears to be more attractive than that of the ORC system.

Due to the change of base engine platform in 2011, a GT Power model (1-D simulation tool) was used to perform a feasibility study of Turbocompound on the long stroke G3500 platform using existing data from multi- and single cylinder engines. A mechanical system with a suitable gear ratio was introduced in the model to send power from the power turbine back to the crankshaft. The simulation showed no significant adverse effects and the results showed that a potential gain of 0.7 to 1.0 points in brake thermal efficiency is possible. The simulation results were shared with the turbocharger supplier. The supplier investigated power turbine options and whether similar efficiency gains could be achieved. The supplier provided two sets of simulation results with appropriate turbines for the first stage and the power turbine.

In 2Q2012, the previous GT-Power simulation model was updated to include a methane oxidation model in the exhaust system. The methane oxidation model will enable additional fuel consumption improvement through the oxidation of unburned fuel in the exhaust system once the charge leaves the cylinder. This moved the brake thermal efficiency gains of the overall system closer to 1 mechanical point. Through the latest iterations in August, it appeared that the overall system is very sensitive to turbine selection. When an engine test cell becomes available, testing on a multi-cylinder with the prototype turbo and appropriate backpressure conditions to mimic the power turbine should confirm this finding.

Two-Stage Intercooled Turbocharging

This project investigated the benefits of a 2-stage inter-cooled compressor to increase compressor efficiency thereby providing improved engine brake thermal efficiency. In 3Q2011, the turbocharger supplier completed a preliminary study and provided new compressor and turbine maps to Caterpillar. Multi-cylinder engine model with the new maps was built for performance validation. Through the rest of the year, Caterpillar continued to work with the turbocharger manufacturer to review simulation estimates. Both parties continued to calibrate the GT-Power model to baseline engine configuration performance. In the beginning of 2012, Caterpillar decided to pursue this technology on a different engine platform; hence, this project was put on hold.

Inlet Valve Actuation Characterization

An Intake Valve Actuation (IVA) system was developed for varying the effective compression ratio on a SCTE. It can be used in a closed loop control to trim the charge pressure to the cylinder to provide improved engine controllability – in terms of both improved steady state stability and improved transient response.

A new design concept was generated and accepted based on performance simulation and hydraulic analysis in 1Q2010. Throughout 2010, preparations for bench testing the IVA parts and the control system were underway and parts procurement was in the final stage. In 2Q2010, a test bench was built and commissioned and the IVA system performance was evaluated on the bench. Cylinder tests were conducted with the IVA on board in 1Q2011. Its ability to improve engine efficiency by balancing cylinder pressure across multiple cylinders, change individual cylinder load and control engine speed were measured. Tests indicated that a benefit of over 0.5% point in engine efficiency is possible by balancing the cylinder pressure of multiple cylinders. The IVA system also showed excellent repeatability of valve closing timing of +/- 0.5 deg CA and was able to hold speed at least equal to or better than that of the throttle.

In 2011, it was determined that Caterpillar gas engines in the future may deploy hydraulic lash adjusters and would result in a fundamental change to the IVA design which operates with a nominal valve lash. This project was therefore put on hold.

Cylinder Head, Piston, and Liner Development

Reciprocating engine frictional losses have been quantified in the DOE funded Light Truck Clean Diesel (LTCD) program. Work in this program concluded that the largest loss is from the sliding contact between the piston and the liner, which agrees with automotive engine research findings. Their work has also quantified the friction reduction associated with utilizing a steel piston as compared to an aluminum piston. This result can be applied directly to large natural gas engines. Steel should also provide opportunities to improve efficiency by reducing thermal losses from the combustion chamber. The use of an alternative liner configuration may allow reductions in crevice volumes. Reductions in crevice volumes would allow improvements in efficiency by forcing more of the fuel in the crevices to enter the combustion in the main chamber. This additional fuel utilization would also lead to significant reductions in methane emissions, reducing the greenhouse gas emissions of the engine. FEA and CFD were used in mid-2009 to evaluate possibilities for improved pistons and liner. The new piston would allow cylinder pressure and BMEP increases, improving efficiency and providing control of heat transfer to allow optimization of crevice features.

The first focus area of this project was to use established internal practices for simulating engine performance with CFD and piston temperature with FEA. This work began during the 2Q2009 and focused on steel piston design through simulation. The second focus area was developing and validating an improved process for performing a combined simulation of the piston cooling gallery (oil gallery) and the combustion space in a single tool to predict piston temperatures for various geometries. This work would make future combustion performance and piston temperature simulations easier by reducing the number of simulation tools and iterations between CFD and FEA. Work during the second quarter on the steel piston design through simulation involved matching combustion simulation results to available data. Baseline piston temperature data was assembled and initial CFD simulations were performed to match predicted combustion performance. Although an issue was found with the code and later corrected, on average this did improve the temperature predictions from FEA compared with measurements but it was not correct at specific locations. In 1Q2010, the process to tune the combustion model and set boundary conditions was revised to match measured cylinder pressure.

The second statement of work was a plan to improve the understanding of the manufacturing process and associated properties of compacted graphite iron (CGI) as a cylinder head material. To insure the best material was chosen for this application, six

materials were chosen for testing: two gray irons, two CGI grades and two ductile grades. Test castings were successfully produced for four of the materials. In 2Q2009, the first phase of testing was completed on all six of the chosen materials. Computer simulations were completed on all materials with two CGI materials proved to the best choice for the combination of properties needed for a cylinder head application. In 4Q2009, all testing including Thermomechanical Fatigue was completed on all materials, except for vibration dampening. The pearlitic CGI proved to have the best fatigue properties at temperatures up to 500C. If a maximum operating temperature of around 400C is experienced, ferritic CGI may provide better life in an engine head. Low Si Gray Iron was an upgrade to current gray iron materials, if the tensile strength could be improved to current gray iron levels. In 1Q2010, Vibration Dampening Testing was performed and as expected gray iron was best, followed by CGI and then ductile iron. Additionally, machinability characterization was also completed. The gray iron was the easiest to machine, followed by ferritic ductile and then pearlitic CGI.

In-Cylinder Feedback

This project studied the methods of sensing detonation as well as optimizing and balancing cylinder-to-cylinder load. Improving the detonation sensing system will allow the engine's timing to be advanced for improved efficiency. The improved system will allow the engine to operate closer to detonation without damage. Balancing and optimizing load will allow improved efficiency and engine output by bringing the load to optimized maximum levels in all cylinders.

In 3Q2009, the sensors and cylinder heads modified to accept the sensors were installed on the Phase-II demonstration engine. The data acquisition system was also installed and tested. In addition, specially modified heads (to allow for both a reference sensor and a test sensor) were installed on a SCTE. Data was collected at different loads and with detonation so that a comparison could be made between the reference pressure sensor, the test pressure sensor and the acoustical knock sensor. Sensors were also placed on a field engine and these sensors were monitored via a wireless remote. At the end of 2Q2010, these sensors had accumulated 2400 run hours. Frequency analysis was used to process the signals from the sensor types on field test and two of the three technologies being tested gave signals that were easily converted to a very accurate knock indicator. The test sensors were removed from the field engine in June, 2011. The sensors were tested against a reference sensor on a hydraulic fixture designed to pulsate a sinusoidal pressure pattern. Sensors were returned to the respective manufacturers for further evaluation. Clark (2011) documented the results of the field test of two sensors, Kistler peizo-electric sensor and Optrand fiber-optic sensor.

Advanced Combustion System

The objective of this project was to improve the thermal efficiency of lean burn gas engine by optimizing the intake port and piston bowl design and to reduce unburned hydrocarbon (UHC) emissions by reducing the valve overlap and delaying the exhaust valve open timing. High turbulence in the combustion chamber may improve the thermal efficiency by increasing the combustion speed (phasing and duration), but it would also have an adverse impact on the thermal efficiency through the increase of pumping and heat losses. This project was to develop an intake swirl port design that would minimize the pumping loss at high swirl ratios and to investigate the impact of piston bowl shape on the in-cylinder swirl flow and combustion efficiency. In 3Q2010, the design iteration using CFD and Design of Experiment was completed and four designs out of 13 candidate port models were selected.

Swirl and mean flow coefficient, Cf, measurement was completed in Caterpillar flow lab. Based on Cf and Swirl ratio, three cylinder head designs were selected to move forward for making actual cylinder heads. The three cylinder heads were manufactured and delivered to Caterpillar in December. The next phase of this project is on engine testing when engine test cell becomes available.

UHC emissions in the industrial lean burn gas engine are primarily composed of unburned methane gases that would have 20-30 times higher greenhouse impact than CO2 emissions and excessive UHC emissions have an detrimental impact on the thermal efficiency as well. Therefore, the reduction of UHC should increase the thermal efficiency of the lean burn gas engine as well as reduce global warming effect. This project investigated the effect of exhaust valve opening timing and valve overlap on the UHC emissions using Fast Flame Ionization Detector (FID) and proposed the best valve timings for reducing UHC emissions. In 4Q2010, preliminary SCTE testing was completed using Fast FID to identify the main source of UHC missions from G3500 gas engine. Five camshafts having different intake and exhaust valve opening and closing timing were designed. The next phase of this project is on engine testing when engine test cell becomes available.

Optimization of Manifold Dynamics

Due to the firing order and the manifold shape, the air charging efficiency of each cylinder in a multi-cylinder engine may be different. The load imbalance between cylinders prevents an engine from achieving maximum performance. Optimization of manifold dynamics will result in performance improvement by reduction of pumping loss and balanced load between cylinders.

In 3Q2011, a process for 1-D & 3-D coupled simulation was successfully established. Meshes for intake and exhaust manifolds were generated. 3-D CFD models were made with the meshes and connected with a 1-D simulation model. The combined model was run for 10~15 cycles in coupled manner, after 30 cycles of 1-D only runs. The result showed detailed distribution of velocity and pressure in the 3-D manifold geometry at each crank angles, as well as transient pressure & mass flux in the whole 1-D engine model. For intake manifold dynamics, the 1-D & 3-D coupled model reproduced load imbalance between odd-numbered and even-numbered cylinders as 1.4 %. It underestimated the measured result, but was higher than the value 0.4% in the 1-D only simulation. For exhaust manifold dynamics, it was found that the 1-D & 3-D coupled model worked similarly with the 1-D only model, because the geometry of the exhaust manifold was so simple that it could be represented by 1-D model relatively easily.

By the end of 2011, several attempts were made to improve accuracy of 1D-3D simulation. A higher order convection scheme was tested and it increased the load imbalance by 0.1 %. Then the mesh resolution effect was tested. To compare with the base mesh (10mm reference size), two sets of more refined meshes (7mm, 5mm reference size) were tried, but the results showed erroneous oscillatory pressure behaviors due to highly skewed mesh quality. The oscillation persisted regardless of changes in time step, connection length and other coupling methods. One more mesh was made more elaborately, and the new mesh (5~7 mm size) did not make oscillation and resulted in an imbalance up to 1.4% in volumetric efficiency and 1.6% in IMEP. The three pressure (cylinder/intake/exhaust) experimental results were examined, and it was found that the 1D-3D simulation gave more realistic pressure trace vs. crank angle in even and odd banks than 1D simulation. The 1D-3D simulation was able to catch the pressure peaks during compression and expansion period, whereas 1D simulation made a different number of pressure peaks. However, the absolute level of imbalance was still far lower than those of the measured values and it was

concluded that the measured imbalance may not be solely caused by the interaction between the firing order and the manifold shape. Since there was still a significant discrepancy between measured IMEP imbalance and CFD simulated one (1.6%), this implied that there may be another reason other than combination of geometry and firing order. With the parametric study on a single cylinder 1-D model, it was suspected that the cam timing might be different by 2.5 deg. CA to reproduce the measured level of IMEP difference. Another 1D-3D calculation was made to validate this assumption, but with different cam angles (valve timing) in LH/RH banks. The result showed that IMEP imbalance increased to 4.4%, a similar level with measured data, but the resulting IMEP pattern still showed discrepancy.

In 1Q2012, another simulation was made for the intake and exhaust coupled case. As the newly released version of the CFD code enabled coupling up to 50 connection points in 1D & 3D model, the 1D-model was connected with a CFD model including both intake and exhaust sides. The simulation produced coupled effect in both sides, but the result was almost similar with the case coupled with intake side only. It was in fact in agreement with the previous result, which showed that 1D + 3D model coupled with exhaust side worked almost identically with the 1-D model because exhaust manifold geometry was relatively simple and was well modeled with 1-D method.

With all of these attempts, it appeared that there were other reasons such as valve timing bias that caused the imbalance. With the assumption that everything else is symmetric, the CFD approach predicted only moderate level of imbalance. Therefore, it was concluded that further CFD analysis was not needed until additional experimental evidence was collected and data to be provided as different input conditions to the CFD model. In 2Q2012, experimental testing to collect pressure in intake and exhaust manifolds and in-cylinder was completed. Preliminary data analysis showed manifold dynamics, manifold geometry and engine hardware are potential root causes of load imbalance.

SCR with On-Board Reductant Generation

SCR technology is a viable option for achieving low NOx emissions, but the cost and complexity of the reductant supply and metering systems make it unattractive. To address these concerns, there was interest in developing an engine-generated reductant. Analysis determined that the Phase-II emissions goal of 0.1g/hp-hr NOx could be achieved with an on-board reductant generation SCR system. Although this resulted in a 4.2% increase in the cost of generated electricity, this still compared favorably to higher cost alternate methods such as 6.9% for urea SCR or 10.2% for reformed fuel technologies. The engine-generated system will also eliminate the fouling and deposit problems associated with urea dosing systems, since a liquid reductant will not be used. The successful demonstration of this technology had spurred interest in determining the production feasibility of the system. A key technical challenge was demonstrating a viable control system to automatically regulate the engine generated reductant.

The primary focus in 1Q2010 was investigating and evaluating options in regards to emission sensor selection, sensor testing, system development instrumentation, test fixturing and scheduling. A gas flow bench was modified to evaluate sensor performance in the lab before conducting on engine tests. Emission and controller instrumentation for supporting system development was identified. In June, 2010, the factory validation tests for the ammonia generation genset (i.e. G3304 engine/generator) were conducted and the generator failed. The problem was traced to a wiring problem with the generator that over stressed and damaged the windings during testing. The generator was returned to the manufacturer with an estimated 3 month delay for replacement. By the end of 2010, a fifty-

hour "break-in" test was successfully completed on the pony genset to verify proper operation and insure stable characteristics before beginning emissions development work. The NOx characteristics in the engine exhaust were mapped over a broad range of air/fuel ratio and load conditions from rich to lean (0.85 to 1.150 lambda) and to access engine governor stability during these conditions. The region of interest was NOx in the 1000 to 4000 ppm range, which was mostly achieved (1000 to 3500 ppm). NOx sensors were modified to accommodate the unusual range required for this project. Sensor performance in the lab was verified to be acceptable (+/-5%) by using a modified test fixture to sweep the 500 to 4000 ppm NOx range and no significant hysteresis was found. In late 2010, this project was placed on hold due to program reprioritization. Project documents, software, and test data was compiled and archived at Caterpillar to facilitate continuation of the work at a later date.

Gasifier Product Gas

During the reformed fuel investigation, hydrogen was shown to extend the lean limit of gas engines. Another more economical source of hydrogen is the product gas of a gasifier. This fuel, either neat or blended with natural gas could provide a greenhouse friendly methane-containing fuel that may also exhibit very good lean (low NOx) performance. This project was to investigate blends of natural gas and simulated gasifier products to determine the performance potential of ARES-class engines on these fuels at CSU Engines and Energy Conversion Laboratory. The modification of the test engine to match the prescribed test method was completed in 2010.

In 1Q2011, the design of fuel blending system was completed and finalized. Key components of this system including flow meters, pumps, and controllers for fuel blending and CFR engine test were procured. The engine and fuel blending system was assembled. Hardware and software debugging was completed in 3Q2011 and the spark timing and A/F sweep test at different load and compression ratio with natural gas was run. After the engine overhaul in 4Q2011 that included an engine tear down, valve/seat clearance measurement, and liner and piston inspection, hardware and software development for the detonation test in CFR engine was completed in the beginning of 2012. In June, CSU successfully completed MN test for 35 syngases selected from customer. MN program was developed using the MN measured experimentally and is being used in Caterpillar to rate the engine performance for various syngas produced in the customer sites.

Experimental and Numerical Determination of Laminar Flame Speed of Syngas

Caterpillar gas engine has successfully demonstrated its capabilities to produce electricity using the syngas fuel made from renewable feedstock through field demonstration and the engine performance test in the lab. However, limited knowledge on the syngas combustion makes it difficult to utilize current sophisticated simulation tools to predict the engine performance and optimize the hardware and software for high thermal efficiency and high power density. This project was to conduct a fundamental combustion study on syngas combustion and to develop chemical kinetic model for predicting combustion characteristics of syngas at high pressure and lean condition through the collaboration with the combustion lab in the University of Southern California (USC). Phase 1 was largely an experimental determination of laminar flame speed of specified syngases in the modest pressure range (up to 5 atm). The goals for phase 2 were:

- Experimentally determining laminar flame speeds at high pressures (up to 40 atm) to validate and optimize the chemical kinetics

- Determination of flammability and detonation/knocking limits at high pressures
- Providing insight into the mechanisms controlling the limit of operations of the various syngas fuels and development of mixing rules

Phase 1: Table 1 shows the detailed composition of the syngas fuels that were studied. The data would form a database that could be used subsequently to evaluate the adequacy of current combustion reaction model. Such data and model are not currently available.

		1st Syngas	2nd Syngas	3rd Syngas	4th Syngas	5th Syngas
Test Gas Composition	H_2	39%	18%	26%	50%	50%
	CO	37%	18%	12%	20%	20%
	CH_4	0%	2%	45%	0%	15%
	CO_2	17%	14%	6%	15%	0%
	N_2	7%	48%	11%	15%	15%

Table 1. Composition of Syngas Fuel

By the end of 2011, both aerodynamically shaped burners and straight-tube burners can produce flows with top-hat velocity profiles and result in planar flames. Aerodynamically shaped burners were used in the atmospheric pressure rig, while straight burners were used in the high-pressure rig. For the flame propagation studies, the twin-flame technique was used, by establishing two symmetrical planar nearly adiabatic flames within the nozzle-generated counterflow. Flow field measurements were performed using digital particle image velocimetry (DPIV), and the flow was seeded with 0.3 μm diameter silicon oil droplets that are produced by a nebulizer. DPIV provides a high temporal and spatial resolution of the instantaneous flow field by tracking the spatial displacement of particles. The seeded particles were illuminated by a double-pulsed laser light within a short time interval, and the light scattered by the illuminated particles is captured by a high quality charged couple devices (CCD) camera. A dual head Nd:YAG laser provided the light source for the flow field illumination and a high performance digital 12 bit CCD camera with 1392 × 1024 pixels of resolution was used to acquire the DPIV images. The Nd:YAG laser has two resonators and is frequency doubled, to achieve light with a wavelength of λ= 532 nm. A Thorlabs® FL-532-3 bandpass (laser line) filter is used to filter out light generated by the flame, and only captures on the camera sensor light generated by the flow seeding particles illuminated by the laser. Figure 2 depicts the general schematic used for the experiments.

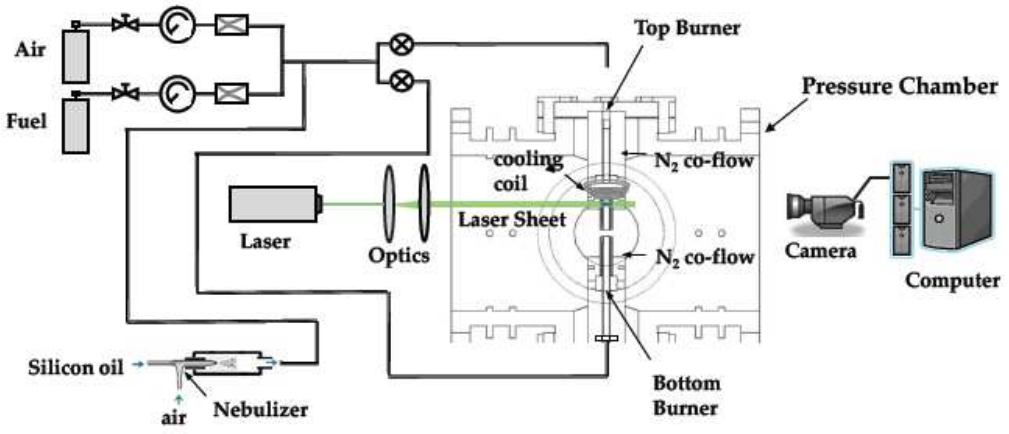

Figure 2. Schematic of the experimental configuration

Laminar flame speeds, S_u^o, were determined using the twin flame configuration. Two symmetrical and planar flames were established between the counterflow burners. The minimum axial flow velocity upstream of the flame was defined as the reference flame speed, $S_{u,ref}$, and the maximum absolute value of the velocity gradient upstream of the flame is defined as the strain rate, K. S_u^o was determined through non-linear extrapolation of $S_{u,ref}$ to K = 0 using a computationally-assisted approach developed recently by the Principal Investigator. The counterflow configuration has been used extensively to determine laminar flame speed using linear extrapolation of the reference flame speed to zero strain. At a given ϕ and nozzle separation distance the $S_{u,ref}$ variation with K was determined numerically using the opposed jet flow code. The value of the laminar flame speed was then determined using the PREMIX flame code for this ϕ. The computed $S_{u,ref}$ vs. K trend was fitted using appropriate polynomials and the experimentally determined S_u^o was determined at K = 0. It is hypothesized that the shape of the computed curve provides a close approximation for the non-linear behavior of the reference flame speed at K's, as shown in Figure 3.

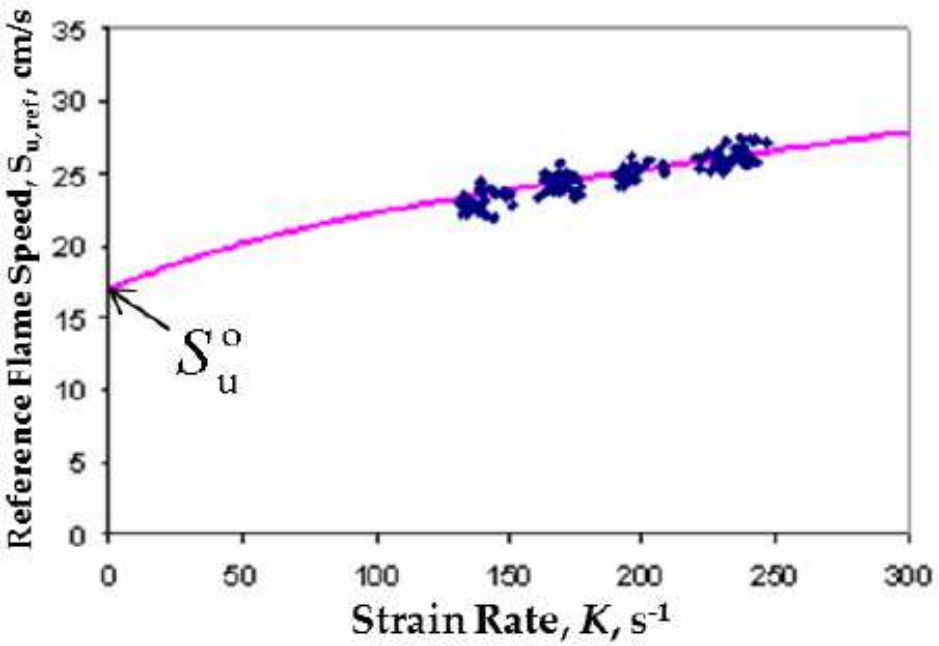

Figure 3. Non-linear extrapolation of reference flame speed against strain rate

Spherically expanding flames, SEF, were studied in a recently developed cylindrical chamber. The chamber is designed to allow for full optical access and a shadowgraph system is in place already. A piezoelectric transducer is used to capture the dynamic pressure rise in the chamber. A picture of the system is shown in Figure 4.

Figure 4. Picture of the constant volume combustion chamber rig

The cylindrical vessel is constructed from 316 SS, measures 220 millimeters in diameter and is 200 millimeters long, and it is fitted with two opposing tungsten electrodes that allow for central point ignition. The shadowgraph system allows for the optical recording of the propagating flames through a CCD camera with the capability of taking pictures up to 8000 frames per second. The images that the camera acquires from the shadowgraph system are very sensitive to density variation, which allows for the identification of the flame as a discontinuity in CCD pixel intensity.

Measurements are conducted by first filling the chamber with the respective fuel and air mixture using the partial pressure method. The mixture is ignited at the center, and at the instant of ignition, the CCD camera is triggered to acquire images of the expanding flame. Using a sensitive image-processing algorithm, a circle is fit and the radius of the expanding flame is determined for each of the images providing the growth of the flame versus time. Using the flame radius vs. time data, laminar flame speeds, S_u^o, were determined (see Appendix B).

Phase 2: Phase 2 of this project studied laminar flame speed of syngas at high pressures and developed a model to determine flammability and detonation limits. In 1Q2012, design of a high pressure chamber for detonation study was completed and laminar flame speed measurement at 10 atm pressure was completed for five syngases. The results were compared with various chemical mechanisms. In 2Q2012, the fabrication of the high pressure chamber for detonation study was completed and the detonation chamber was installed. Laminar flame speed data was measured at 20 atm. Ignition system design for detonation chamber was completed.

During 3Q2012, laminar flame speeds were measured in the cylindrical chamber for pressures ranging from 1 to 35 atm. The experimentally determined laminar flame speeds were computed also using the USC Mech II and GRI 3.0 kinetic models. Comparisons have been made between experimental and computed laminar flame speeds and insight was provided into the mechanisms controlling flame propagation for the fuels shown in Table 1. The GRI 3.0 kinetic model was found to provide closer agreements with our data compared to the more recently developed USC Mech II. The spherical chamber to be used for the detonation chamber was successfully commissioned. The spherical geometry was ideal for studying detonation characteristics. Detonation studies were under way for ambient initial mixture temperature. Mixing rules were developed successfully describing the ignition delays of mixtures of different fuels with air. This development was based on theoretical analysis and detailed numerical simulations. A powerful ignition system has been designed and built, capable of delivering large amounts of energy that was needed to achieve ignition at high pressures and to define experimentally the flammability limits for all fuels.

Organic Rankine Cycle Field Demonstration

A Rankine heat engine is used to extract energy from the exhaust of an Otto cycle engine. The Rankine cycle utilizes an organic material as the working fluid. When used with a G3520C the ORC will produce an additional 18% power with no additional fuel input. The effect is therefore an 18% reduction in brake-specific emissions and a ~6 point improvement in engine efficiency. The lab testing of the prototype ORC 47% efficient performance was demonstrated in 2008.

During 2010, a demonstration project was launched to design an ORC system with production intent incorporating “lessons learned” from the Phase II demonstration. A scope of the project from a system performance, financial, and operation perspective was

developed in 1Q2010. A site selection matrix was also developed to select a site that met the requirements of the project. The heat transfer systems with the outputs of this design used to characterize the overall system performance was designed. A "field demonstration" agreement was developed to address the technical and financial aspects of the project and contract requirements of the DOE and Caterpillar.

In 2Q2010, the project adopted a design philosophy resembling a "kit" which could be added to an existing power plant. The kit was a highly engineered system of commercially available components including the ORC, heat exchangers, pumps, fluid reservoirs, flow control valves, specified pipe sizes etc. The goal of the engineering effort was to minimize project risk while maximizing system performance, financial attractiveness, and operational simplicity. A production ORC system was selected for procurement. Design of the heat transfer systems was underway. The outputs of this design were used to characterize the overall system performance. Throughout the rest of 2010, the ORC field demonstration system team focused on site selection by performing a site viability analysis for a customer in Kentucky. The team completed a system performance prediction for this customer based on current site specifications. All of the equipment for the field demonstration was purchased in 2010. In mid-2011, the project was put on hold due to program prioritization and finally in 3Q2012, this project was cancelled due to the lack of market demand for this technology.

Gasifier Product Gas Demonstration

In January, 2010, NETL and Caterpillar agreed to include a new "opportunity fuel" deliverable that could be funded in 2010. A Caterpillar dealer in the U.S. had sold several gasifiers to customers for industrial heating processes and could arrange to provide an opportunity for us to demonstrate an engine running on the syngas from one of these gasifiers. Following the meeting, successful tests using research engines indicated that a field deployment of gasifier product gas fueled engine could be successful. A site located at Gleason, TN was selected. The local Caterpillar dealer, a brick kiln company having ownership of the site and gasifiers, and the local electric power distributor were engaged for this gasifier product gas demonstration project.

The initial genset specifications were developed and a parts list for the build was finalized. A Caterpillar G3516C having an island mode capability was selected and the fuel system specification was modified to handle high flow rate of gasifier producer gas. The gas clean up skid design including oil and water scrubber was finalized. By the end of 2010, the genset was delivered to the customer site after completing testing in the packaging company. Installation and initial performance checkup of genset on-site were completed in January, 2011 and the commissioning on syngas demonstration system including genset, gasifier, and cleanup skid was initiated.

After first running the system in January, 2011 there were key issues identified in the gas clean-up and control system. A diesel particulate filter was added between the cyclone and the oil scrubber to remove fine particulates from the producer gas before the oil scrubber. After completing the system modification, a second test was conducted during the first week of April and the team was able to run the genset continuously for about 40 minutes with the producer gas. Issues such as fuel pressure instability, debris in the fuel line, fuel temperature control, and humidity control were observed during this trial run. Fuel and oil samples were sent to the lab for the speciation and the engine was torn down for inspection. After the engine was rebuilt, a successful witness test with the Tennessee Valley Authority took place in early August where the genset paralleled with the grid. Process Engineering, an engineering consultant firm, provided a three-phase improvement plan for the gas clean

up skid. The first phase was implemented before the end of 2011 and the engine produced 750 kW, the highest power achieved thus far. Upon the successful start up and commissioning of the syngas unit, ownership of system was transferred to the dealer in August, 2012.

References

Clark, FL. Field Test of Production Intent Cylinder Pressure Sensors. Caterpillar Technical Information Center, DN1063907

Appendix A

Effects of Vibrations on Laser Fiber Delivery System Performance

This experimental setup has similar vibration conditions to what will be used on the engine. The laser source and fiber input are on a vibration isolated platform, while the output end and optical spark plug are mounted on a shaker table representing the vibrating engine cylinder. The shaker table is driven by a variable speed motor at frequencies similar to those of engine operation. To better simulate a prototype engine configuration, fiber connectors on the fiber input and output faces were implemented, allowing quick and easy connection to adjoining hardware. In order to simulate the vibrating environment of an engine in a laboratory test, a Crowson ED-3 bench top shaker table controlled by a laptop computer was used. The shaker was capable of operating anywhere between 5 and 2000 Hz with a maximum amplitude of 6.3 mm. By placing the fiber output end and any required optics on top of the shaker table, engine conditions were mimicked for any frequency and amplitude within the shaker's range of motion. For the tests completed, the shaker operated at 25 Hz, simulating a single cylinder engine at 1500 rpm.

To find ways to dampen vibration without substantial degradation of the fiber output beam quality, it quickly became clear that some form of viscous damping would be beneficial, as it provides a ready means to dissipate energy without imposing large stresses on the fiber. To do this, an oil bath was constructed that would allow us to submerge a large portion of the fiber in oil to dissipate energy. The experimental setup is shown below in Figure A1.

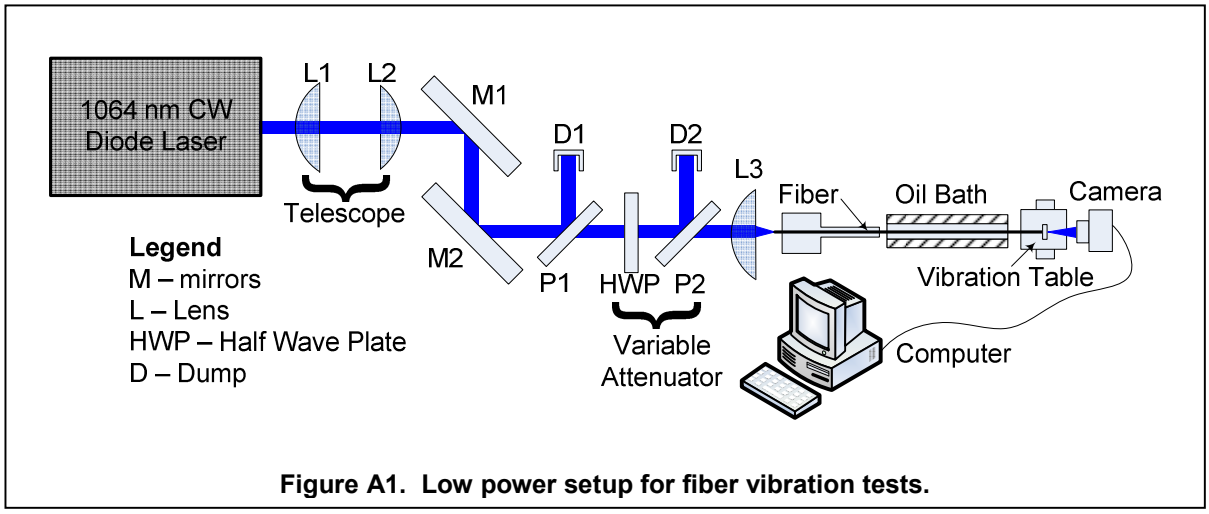

Figure A1. Low power setup for fiber vibration tests.

For all vibration tests performed, 400 μm core, 720 μm clad fibers, approximately 4 m in length were studied. The 4 m length was chosen because it is practical for large engine usage. The fibers were polished and a standard connector was attached to the output end. The connector end was attached to the shaker table, and the beam could be imaged using a CCD camera. The camera was used with a very short exposure time to capture ("freeze") the moving output beam, with a variable attenuator to help control the power incident on the CCD chip. Images were captured at about 25 frames per second, so that the beam could be imaged at one particular position along its motion or at multiple points along its motion.

Stationary beam quality tests showed that the best possible output with the test fiber is an M^2 of approximately 4.0. In the initial test setup, in order to immerse the fiber in the oil, the fiber had to be bent (draped) down into the bath. The need to bend the fiber in a discontinuous manner caused increased stress and degraded the stationary (vibration free)

beam quality to M^2=5.8. However, the viscous damping was shown to benefit the fiber beam quality. As shown in Figure A2, the oil immersion improves the beam quality (reduces the M^2 parameter) in the vibrating case.

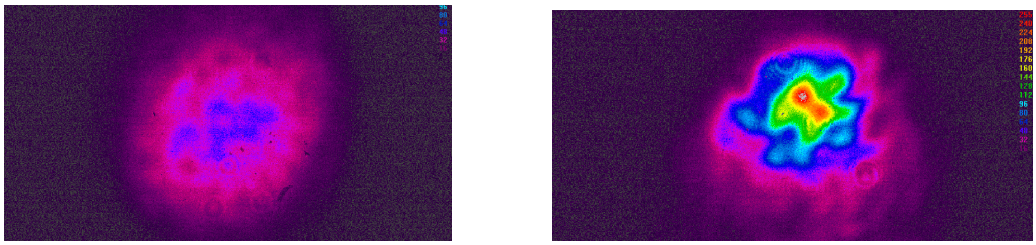

Figure A2. Beam profiles from vibration tests. Left: Fiber vibrating in oil bath with no oil (M^2=8.1). Right: Fiber vibrating in oil bath with oil (M^2=6.5).

To test the ability of the fiber in the oil bath to create sparks, the experiment was instead conducted with a high-power pulsed 1064 nm laser, operating at 10 Hz. The setup is similar but with a pulsed laser as the light source and focusing optics (for spark formation) at the output end. In this case, the fiber connector was attached to an adjustable mount on a cage system that also contained a collimating lens, the focusing lens (10 mm focal length Gradium lens), and a pressure cell. This entire system sat on the shaker table, simulating what will eventually be needed for an optical plug on an engine. The variable attenuator controls the power incident on the fiber input, and the same oil bath was used. The assembly of focusing optics and pressure cell, positioned on the shaker table, is shown in Figure A3.

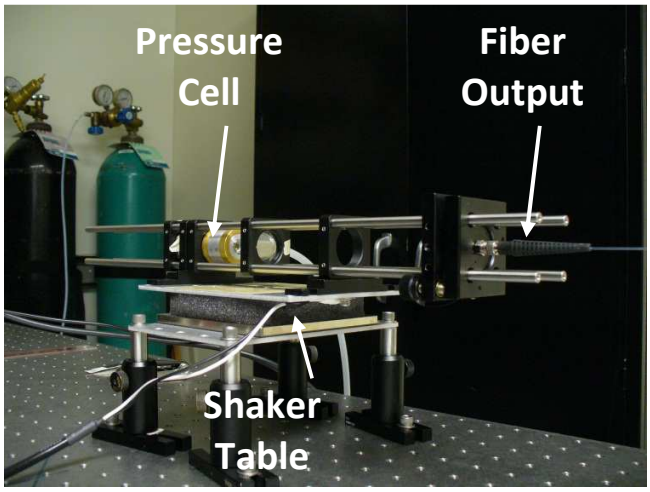

Figure A3. Shaker table with cage system.

While this experiment still has some issue with misalignment and degradation, initial results have shown 100% reliable sparking while vibrating at 25 Hz and for cell pressures of 13.6 and

6.8 bar gauge (200 and 100 psig). With the fiber in the oil bath, laser output pulses of energy 14 mJ and duration 50 ns allowed reliable (100%) spark formation.

Appendix B

The experimental and computed S_u^o

The experimental and computed S_u^o's are shown in Figures B1-B10; note that in all figures, symbols correspond to the experimental data and lines to computations.

Syngas #1 – Counterflow Flames

Figure B1 depicts the results for Syngas #1 (39%H2 -37%CO -0%CH4 -17%CO2 -7% N2) at p = 1 atm. The computed S_u^o's are slightly lower than the data as ϕ approaches unity.

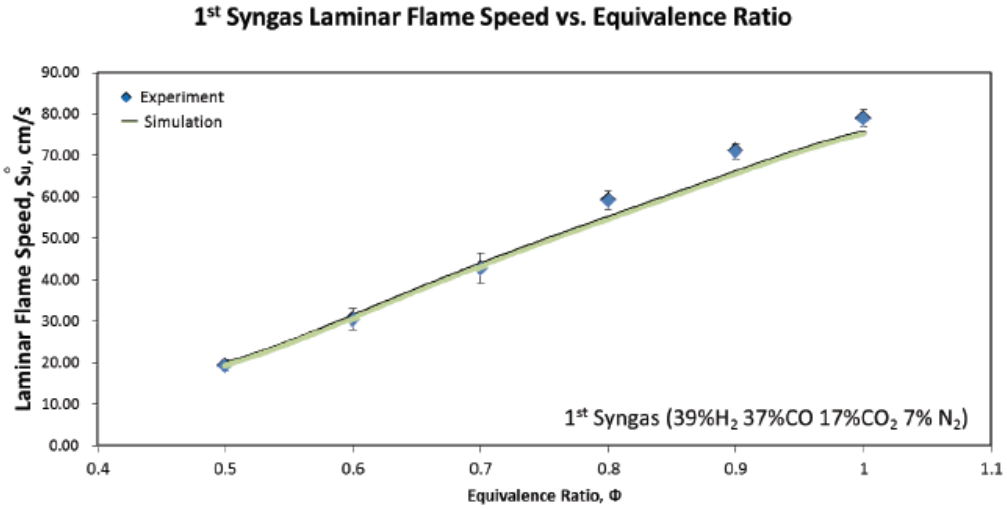

Figure B1. S_u^o's of Syngas #1 at p = 1 atm.

Figure B2 depicts the results for Syngas #1 at p = 5 atm. The N_2 to O_2 molar ratio chosen for this syngas is 87:13. The predictions are in good agreement with the data for flame temperatures above 1500 K.

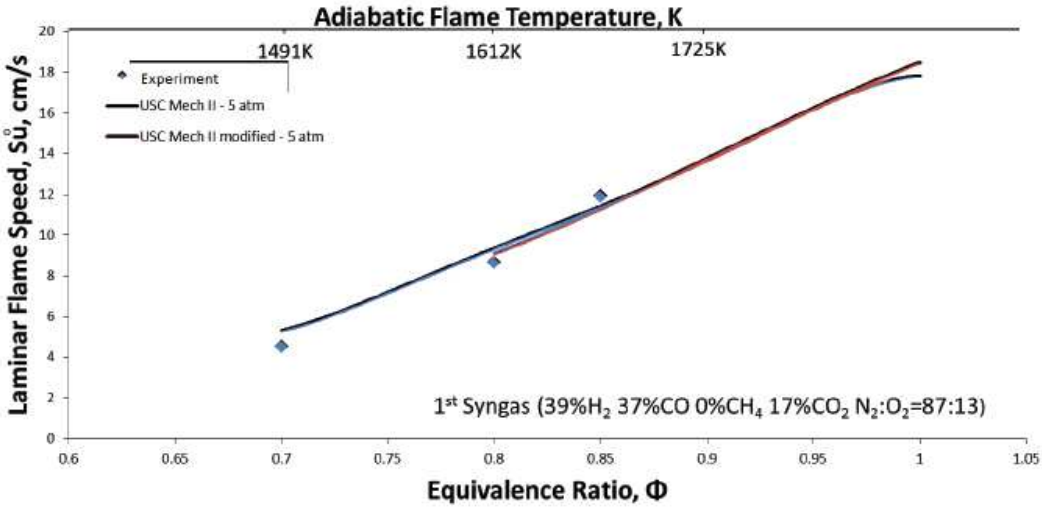

Figure B2. S_u^o's of Syngas #1 at p = 5 atm.

Syngas #2 – Counterflow Flames

Figure B3 depicts the results for Syngas #1 (18%H2 -18%CO -2%CH4 -14%CO2 -48% N2) at p = 1 atm. The computed S_u^o's are slightly lower than the data as ϕ approaches unity.

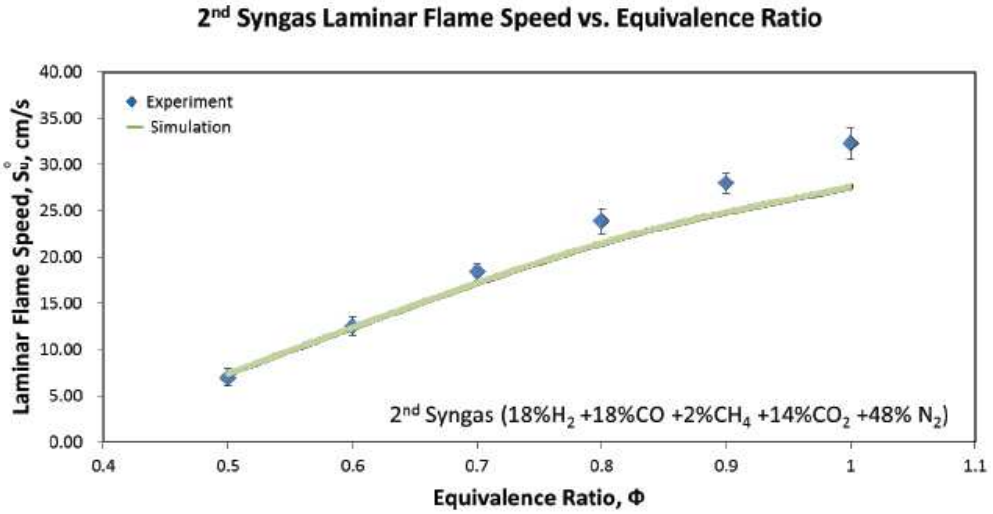

Figure B3. S_u^o's of Syngas #2 at p = 1 atm.

Figure B4 depicts the results for Syngas #2 at p = 5 atm. The N_2 to O_2 molar ratio chosen for this syngas is 86:14. The predictions are higher than the data for flame temperatures below 1500 K.

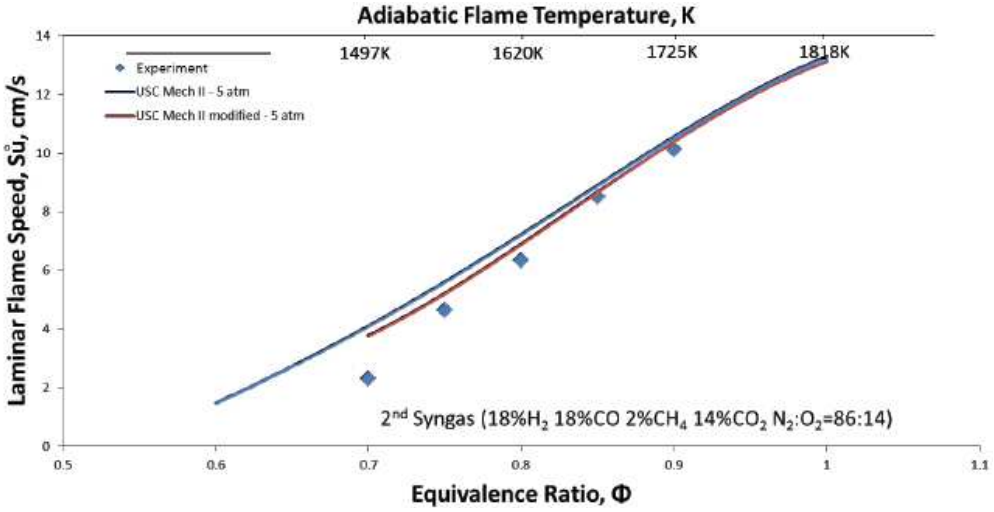

Figure B4. S_u^o's of Syngas #2 at p = 5 atm.

Syngas #3 – Counterflow Flames

Figure B5 depicts the results for Syngas #3 (26%H2 -12%CO -45%CH4 -6%CO2 -11% N2) at p = 1 atm. The computed S_u^o's are slightly lower than the data as ϕ approaches unity.

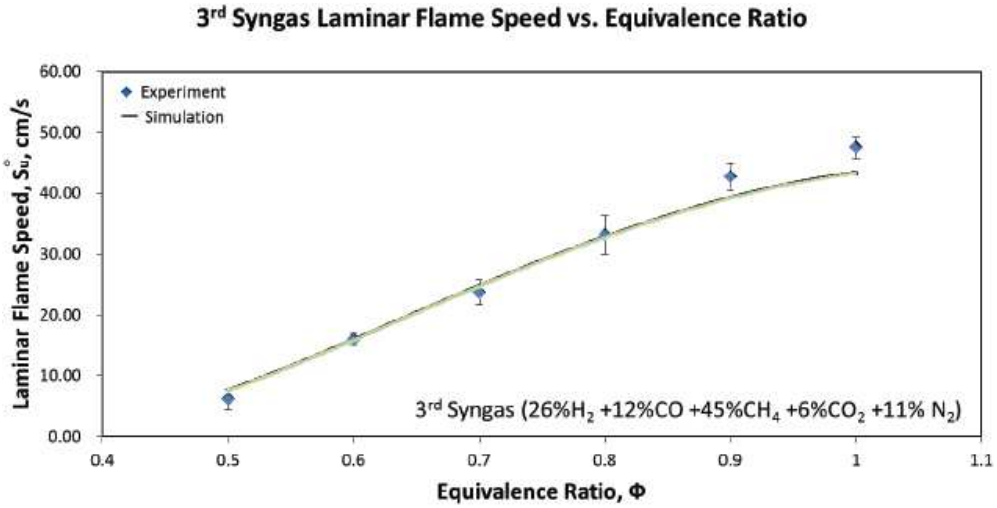

Figure B5. S_u^o's of Syngas #3 at p = 1 atm.

Figure B6 depicts the results for Syngas #3 at p = 5 atm. The N_2 to O_2 molar ratio chosen for this syngas is 82:18. The predictions by both models are higher than the data for all conditions. Note that in Syngas #3, CH4 exists in high quantities.

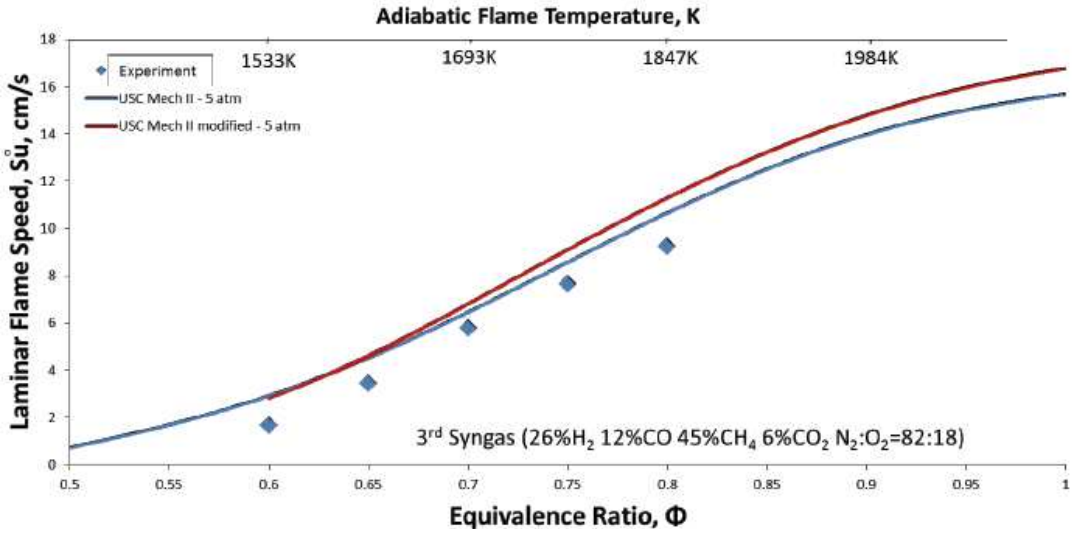

Figure B6. S_u^o's of Syngas #3 at p = 5 atm.

Syngas #4 – Counterflow Flames

Figure B7 depicts the results for Syngas #4 (50%H2 -20%CO -0%CH4 -15%CO2 -15% N2) at p = 1 atm. The computed S_u^o's are slightly lower than the data as ϕ approaches unity.

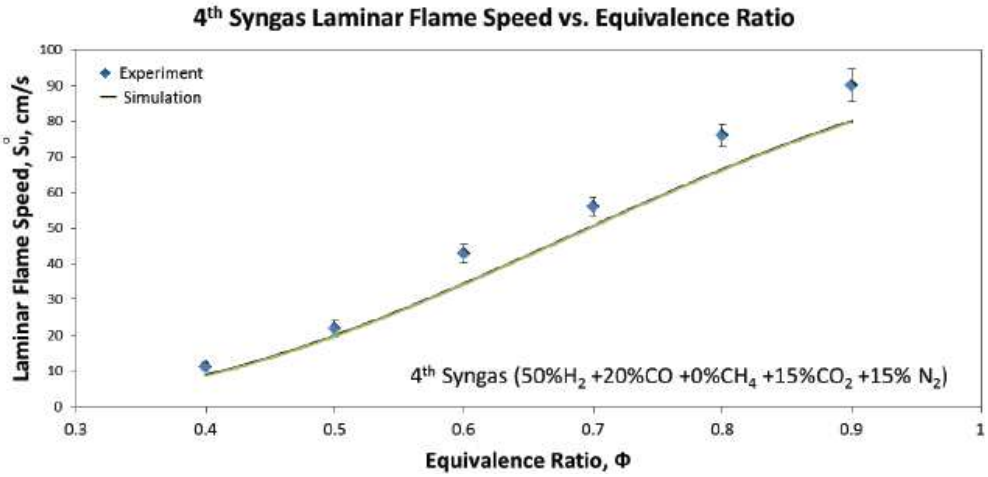

Figure B7. S_u^o**'s of Syngas #4 at p = 1 atm.**

Figure B8 depicts the results for Syngas #4 at p = 5 atm. The N_2 to O_2 molar ratio chosen for this syngas is 88:12. The predictions by both models are higher than the data for all conditions. The higher amount of N_2 was required as the H_2 content is high and thus the attendant laminar flame speeds are higher.

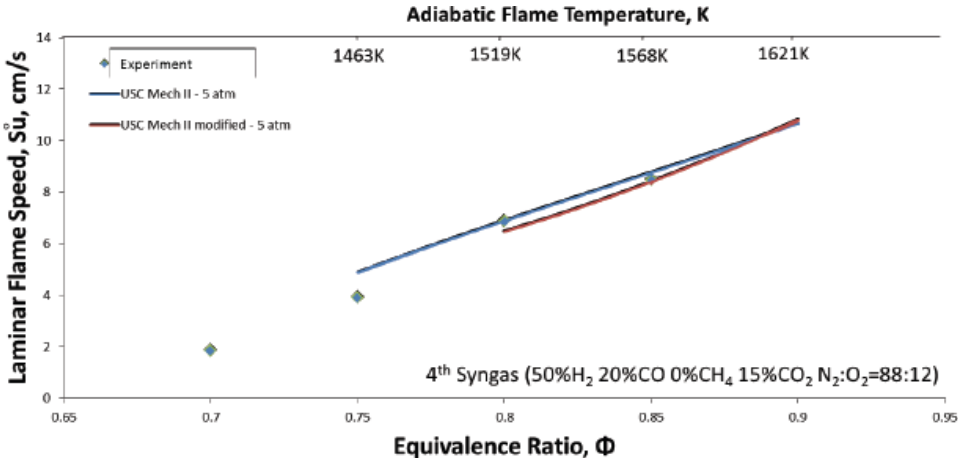

Figure B8. S_u^o**'s of Syngas #4 at p = 5 atm.**

Syngas #5 – Counterflow Flames

Figure B9 depicts the results for Syngas #5 (50%H2 -20%CO -15%CH4 -0%CO2 -15% N2) at p = 1 atm. The computed S_u^o's are slightly lower than the data as ϕ approaches unity.

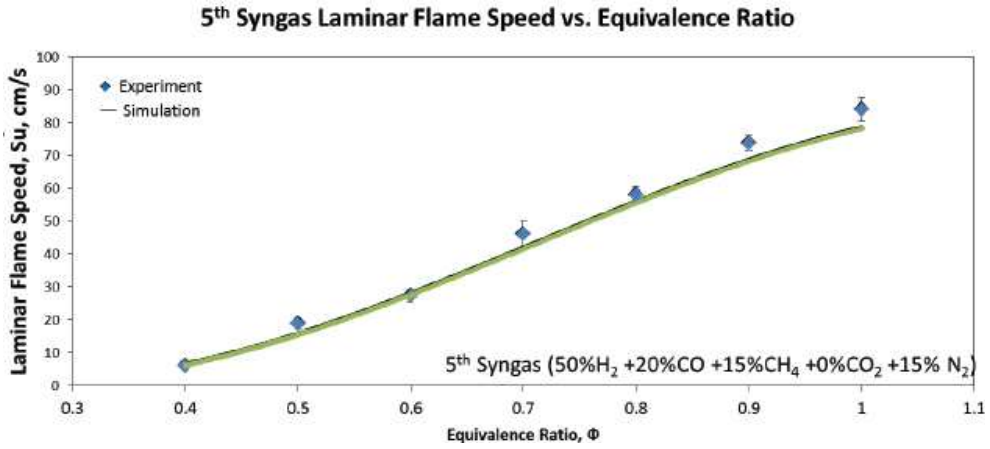

Figure B9. S_u^o's of Syngas #5 at p = 1 atm.

Figure B10 depicts the results for Syngas #5 at p = 5 atm. The N_2 to O_2 molar ratio chosen for this syngas is 88:12. The predictions by both models are higher than the data for all conditions. Similar to Syngas #4, the higher amount of N_2 was required as the H_2 content is high and thus the attendant laminar flame speeds are higher.

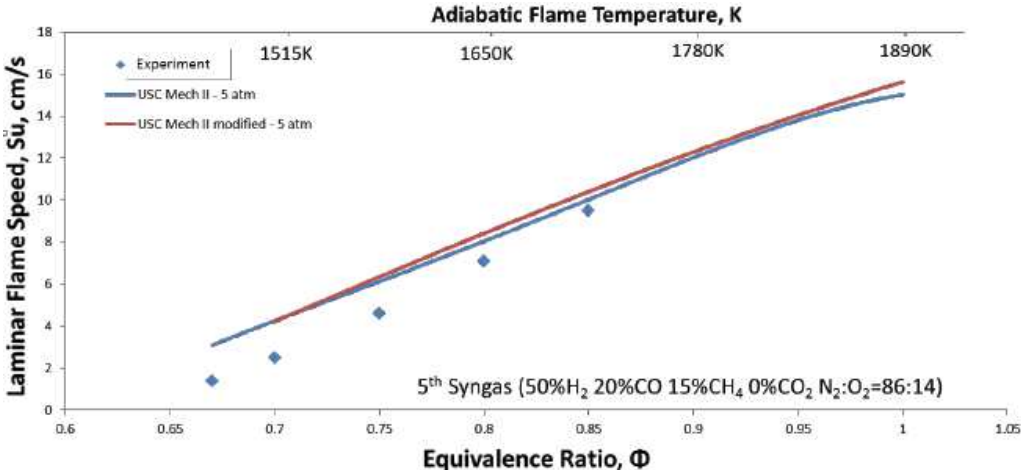

Figure B10. S_u^o's of Syngas #5 at p = 5 atm.

Syngas #3 and 5 – Spherically Expanding Flames

Figures B11 and B12 depict preliminary results for Syngas #3 and #5 at p = 2, 5, and 7 atm. The computed S_u^o's are slightly lower than the data as ϕ approaches unity. The data were taken at relatively high flame temperatures and the agreements with the modeling results are rather close. In these experiments, Helium had to be used as diluent to suppress thermo-diffusional instabilities at low strain rates at which the data were taken.

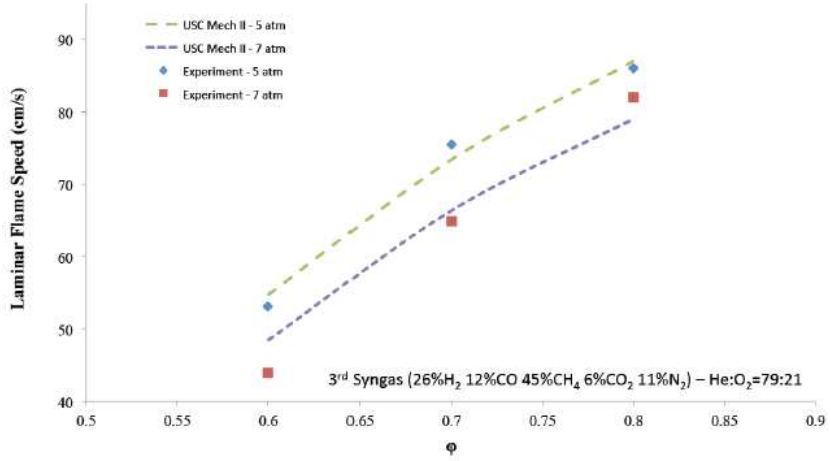

Figure B11. S_u^o**'s of Syngas #3 at p = 5 and 7 atm.**

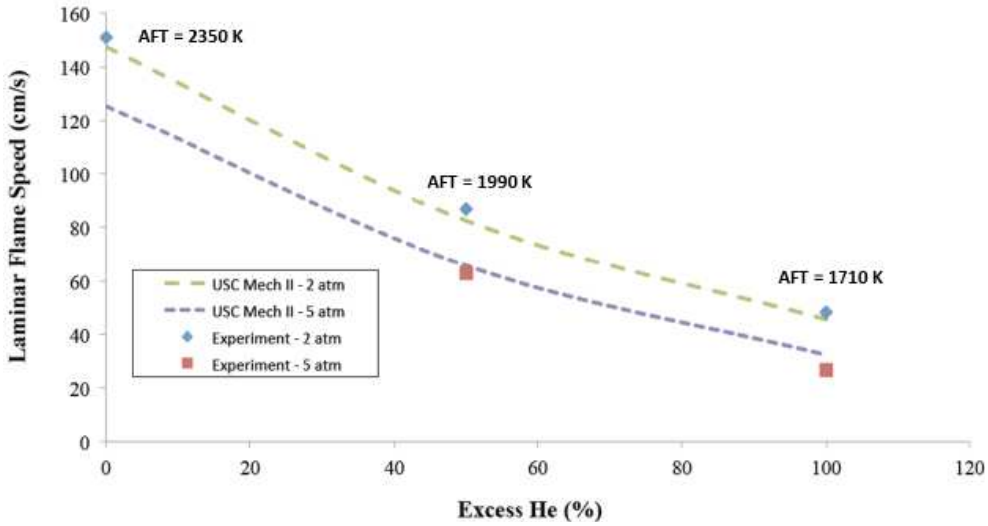

Figure B12. S_u^o**'s of Syngas #5 ϕ= 0.7 at p = 2 and 5 atm.**
(*AFT stands for Adiabatic Flame Temperature)